ELSEVIER

Quaternary Science Reviews 26 (2007) 1790–1809

QSR

Understanding the origin and analysis of sediment-charcoal records with a simulation model

Philip E. Higuera[a,b,*], Matthew E. Peters[c,d,1], Linda B. Brubaker[a], Daniel G. Gavin[e]

[a]*College of Forest Resources, University of Washington, Seattle, WA, USA*
[b]*Department of Earth Sciences, Montana State University, Bozeman, MT, USA*
[c]*Department of Applied Mathematics, University of Washington, Seattle, WA, USA*
[d]*Department of Atmospheric Science, University of Washington, Seattle, WA, USA*
[e]*Department of Geography, University of Oregon, Eugene, OR, USA*

Received 23 June 2006; received in revised form 15 March 2007; accepted 21 March 2007

Abstract

Interpreting sediment-charcoal records is challenging because there is little information linking charcoal production from fires to charcoal accumulation in lakes. We present a numerical model simulating the major processes involved in this pathway. The model incorporates the size, location, and frequency of fires, primary and secondary charcoal transport, sediment mixing, and sediment sampling. We use the model as a tool to evaluate assumptions of charcoal dispersal and taphonomy and to assess the merits of inferring local and regional fire history by decomposing charcoal records into low-frequency ('background') and high-frequency ('peak') components. Under specific dispersal scenarios, the model generates records similar in appearance to sediment-charcoal records from Alaskan boreal forests. These scenarios require long-distance dispersal (e.g. 10^0–10^1 km), consistent with observations from wildfires but longer than previously inferred from experimental dispersal data. More generally, charcoal accumulation in simulated records mainly reflects area burned within the charcoal source area. Variability in charcoal peak heights is primarily explained by the size of charcoal source areas relative to the size of simulated fires, with an increase in this ratio resulting in increased variability in peak heights. Mixing and multi-year sampling add noise to charcoal records, obscuring the relationship between area burned and charcoal accumulation. This noise highlights the need for statistical treatments of charcoal records. Using simulated records we demonstrate that long-term averages of charcoal accumulation ($>10\times$ mean fire return interval) correlate well with area burned within the entire charcoal source area. We further demonstrate how decomposing simulated records to isolate the peak component emphasizes fire occurrence at smaller spatial scales (<1 km radius), despite the importance of long-distance charcoal dispersal in simulating charcoal records similar to observations. Together, these results provide theoretical support for the analysis of charcoal records using the decomposition approach.

1. Introduction

Interpreting fire history from sediment charcoal records depends upon understanding the processes controlling charcoal accumulation and the use of analytical methods that appropriately reflect these processes. Over the past two decades, a number of empirical and theoretical studies has helped identify key assumptions about charcoal-dispersal and other taphonomic processes affecting sediment charcoal records (Wein et al., 1987; Clark, 1988; MacDonald et al., 1991; Clark and Royall, 1995a; Bradbury, 1996; Whitlock and Millspaugh, 1996; Clark and Patterson, 1997; Clark et al., 1998; Blackford, 2000; Mohr et al., 2000; Carcaillet et al., 2001b; Lynch et al., 2004a; Whitlock et al., 2004; Higuera et al., 2005). These assumptions provide a rationale for analytical frameworks used to interpret fire occurrence from continuous records of macroscopic charcoal[2] (e.g. Clark, 1988, 1990; Clark et al., 1996; Long et al., 1998; Carcaillet et al., 2001a; Gavin et al., 2003,

*Corresponding author. Department of Earth Sciences, Montana State University, Bozeman, MT, USA. Tel.: 1 406 599 8908; fax: 1 406 994 6923.
E-mail address: philip.higuera@montana.edu (P.E. Higuera).
[1]Current address: Department of Earth and Planetary Sciences, Harvard University, Cambridge, MA, USA.

[2]Unless otherwise noted, "charcoal" refers to macroscopic charcoal particles, typically those $>100\,\mu$m in diameter.

0277-3791/$ - see front matter © 2007 Elsevier Ltd. All rights reserved.
doi:10.1016/j.quascirev.2007.03.010

2006). Nevertheless, evaluating the assumptions of charcoal analysis and developing appropriate analytical techniques remain two important research goals for interpreting the characteristics and variability of past fire regimes (Whitlock and Anderson, 2003). Modeling sediment charcoal records provides a tool that can help in both respects. Here we describe a model that translates the current understanding of charcoal dispersal and taphonomy into a numerical framework that simulates lake sediment-charcoal records. Assumptions of charcoal analysis are evaluated by comparing simulated records to empirical records from Alaskan lakes, and the merits of analytical approaches are examined by comparing simulated charcoal records with the known (simulated) fire histories that created them.

The interpretation of fire history from sediment charcoal rests upon three main assumptions about charcoal taphonomy (dispersal and secondary transport) and sampling. First, most macroscopic charcoal falls close to its source, such that peaks in sedimentary charcoal represent "local" fire occurrence. This assumption was considered by Clark (1988), who used a Gaussian plume model to argue that macroscopic charcoal should be deposited within 10^1–10^3 m of its source. Studies of charcoal deposition from experimental fires are consistent with these theoretical considerations and suggest that "local" could be defined as within several tens to hundreds of meters of a sedimentary basin (Wein et al., 1987; Clark et al., 1998; Blackford, 2000; Ohlson and Tryterud, 2000; Lynch et al., 2004a; Peters and Higuera, 2007). This spatial scale is also supported by studies matching charcoal peaks to known fire events (e.g. Clark, 1990; Whitlock and Millspaugh, 1996; Gavin et al., 2003; Lynch et al., 2004a; Higuera et al., 2005). On the other hand, several studies have shown that macroscopic charcoal can travel several to tens of kilometers away from wildfires (Pisaric, 2002; Tinner et al., 2006) and create distinct charcoal peaks in sediment records (Whitlock and Millspaugh, 1996; Gardner and Whitlock, 2001; Hallett et al., 2003). Recent theoretical work considering charcoal dispersal in two dimensions (Peters and Higuera, 2007) also argues against the extremely short dispersal distances (e.g. <100 m) suggested by some experimental fires (Clark et al., 1998; Ohlson and Tryterud, 2000; Lynch et al., 2004a). The feasibility and unknown impacts of such widely varying dispersal distances make the spatial scale of sediment charcoal records difficult to understand.

Second, interpreting fire history from charcoal stratigraphy assumes that secondary charcoal deposition via slope wash or within-lake redeposition does not obscure patterns of primary charcoal deposition. This assumption is supported by the physical properties of macroscopic charcoal (size, shape, and density), which suggest that redistribution across the landscape should be minimal (Clark, 1988; Clark and Patterson, 1997; Clark et al., 1998; Lynch et al., 2004a). In addition, empirical work indicates that post-fire erosion in boreal forests of Eastern North America is minimal (Carcaillet et al., 2006) and charcoal peaks from known fires remain distinct despite within-lake redistribution of charcoal in non-fire years (Bradbury, 1996; Whitlock and Millspaugh, 1996). Thus, existing evidence indicates that primary charcoal deposition should remain the dominant signal in charcoal records, in at least some sedimentary basins.

Third, interpreting fire occurrence assumes that sediment mixing and sampling provide adequate temporal resolution for detecting local fire occurrence (Whitlock and Larsen, 2001). Clark (1988) used a simple sediment mixing model to suggest that sampling intervals should be <0.2 times the fire-return-interval of interest to resolve individual charcoal peaks (i.e. yr sample$^{-1} \leqslant 0.2$ yr fire^{-1}).

From these assumptions comes the rationale for analyzing charcoal records by decomposing a charcoal series (C_{raw}) into "background" ($C_{background}$) and "peak" (C_{peak}) components (e.g. Clark et al., 1996; Long et al., 1998; Carcaillet et al., 2001a; Lynch et al., 2002; Gavin et al., 2003). Clark and Royall (1995b) originally used the terms "background" and "peak" to discriminate between the low-frequency trends in abundant, small charcoal (<100 μm diameter) and higher-frequency trends in less abundant, large charcoal (>100 μm diameter). Clark and co-authors emphasized the different spatial scales of these components: peak and background charcoal represent local and regional source areas, respectively (Clark and Royall, 1995a; Clark et al., 1996; Clark and Patterson, 1997). Long et al. (1998) applied these terms to purely macroscopic charcoal records and expanded the definition of background to include the effects of charcoal production per fire and secondary charcoal transport, which could change with changing vegetation and geomorphic regimes. Thus the term "background" has been used differently in the literature to account for both ecological and physical processes that can cause low-frequency variations in sediment charcoal accumulation. Peak charcoal is assumed to represent primary charcoal deposition from "local" fires and analytical and naturally occurring noise from all sources of charcoal deposition. A threshold separates charcoal samples representing noise from those mainly representing "local" fires.

In this paper, we describe a numerical model (the Charcoal Simulation Model, CharSim) developed as a tool for evaluating assumptions of charcoal dispersal and taphonomy and for assessing the merits of analytical techniques for inferring fire history. Through model description and comparisons between simulated and Alaskan sediment charcoal records, we illustrate the major processes creating variability in sediment charcoal records. We use comparisons between simulated records and their underlying fire histories to assess the impacts of different taphonomic and analytical scenarios on interpretations of fire history using the decomposition approach.

2. Methods and rationale

2.1. The charcoal simulation model

CharSim simulates and links (1) the spatial and temporal pattern of fire regimes, (2) charcoal production, dispersal,

Table 1
Components of the Charcoal Simulation Model (CharSim) include the major processes linking fires on a landscape to the creation of a sampled sediment charcoal record

Component	Details and/or parameters	Primary references	Secondary references
1. Fire regime	(a) Mean number of fires per year (Poisson probability) (b) Mean and variance of log-transformed fire-size distribution (i.e. log-normal probability)	(a) Kasischke et al. (2002), Higuera (2006) (b) Alaska Fire Service (2004)	(a) Lynch et al. (2002, 2004b)
2. Charcoal production, dispersal, and primary deposition	(a) Charcoal production (b) Charcoal dispersal (c) Mean fall speed (d) Mode and variation of injection heights (e) Wind speed (f) Wind direction	(a) Estimated (b) Peters and Higuera (2007) (c) Lynch et al. (2004a) (d) Estimated, see Peters and Higuera (2007) (e) Taylor et al. (2004) (f) Instrumental wind data[a]	(a) Clark et al. (1998)
3. Secondary charcoal deposition	(a) Proportion and temporal pattern of landscape-derived charcoal (b) Proportion and temporal pattern of within-lake redeposition	(a) Estimated (b) Estimated	(a, b) Bradbury (1996), Carcaillet et al. (2006), Whitlock and Millspaugh (1996), Clark and Patterson (1997)
4. Sediment mixing	(a) Mean mixing depth (b) Mixing distribution (c) Sediment accumulation rate	(a–c) Higuera (2006), estimated	
5. Sediment sampling	(a) Sampling resolution	(a) Higuera (2006)	
6. Fire history interpretation	(a) Correlation between CHAR and area burned (b) Maximum accuracy	(a) This paper (b) This paper	

Primary references provided quantitative values, while secondary references provided either additional support or qualitative information from which estimates were based.
[a]Bettles, Alaska, 1971–2000: Alaska Climate Research Center, http://climate.gi.alaska.edu/Climate/Wind/Direction/Bettles/BTT.html.

and primary deposition, (3) secondary deposition, (4) sediment mixing, and (5) sediment sampling (Table 1). Each component is potentially important in creating sediment-charcoal records, although some processes are difficult to parameterize due to a lack of empirical data. We parameterized CharSim to represent fire regimes and macroscopic charcoal records in lake sediments from interior Alaska, an area dominated by black spruce boreal forest and large, high-severity fires (e.g. Kasischke et al., 2002). The model code (MatLab Version 7.0.0 and C) is available from the authors upon request.

The following sections describe the processes contained within any conceptual model of charcoal production, transport, and deposition, the components and design of CharSim, and the technical details of the model. Fig. 1 illustrates each step of the model, from airborne charcoal deposition to charcoal in a sampled sediment core.

2.1.1. Fire regime

CharSim simulates burning on a homogenous landscape represented by 100×100 m (1 ha) pixels. Fires start within a circular "study area" of 50-km radius (i.e. 78,540 km^2 area) with a "lake" at its center (represented by a single 1-ha pixel). The number of fires occurring in any year is determined by a Poisson probability distribution with a prescribed mean number of fires per year (λ). Fires start at random locations on the landscape and grow to a size based on a normal probability density function (PDF) fit to log-transformed fire sizes from Alaska ($n = 1058$, 1988–2003 data; Alaska Fire Service, 2004; Table 1). The size of each fire, FS_i, is randomly selected from this PDF. The minimum and maximum fire size recorded in the Alaskan dataset are 11 and 236,128 ha, so the spatial extent of CharSim can include $>99\%$ of the fire sizes contained within the Alaskan-derived fire-size distribution. Fires grow in a circular

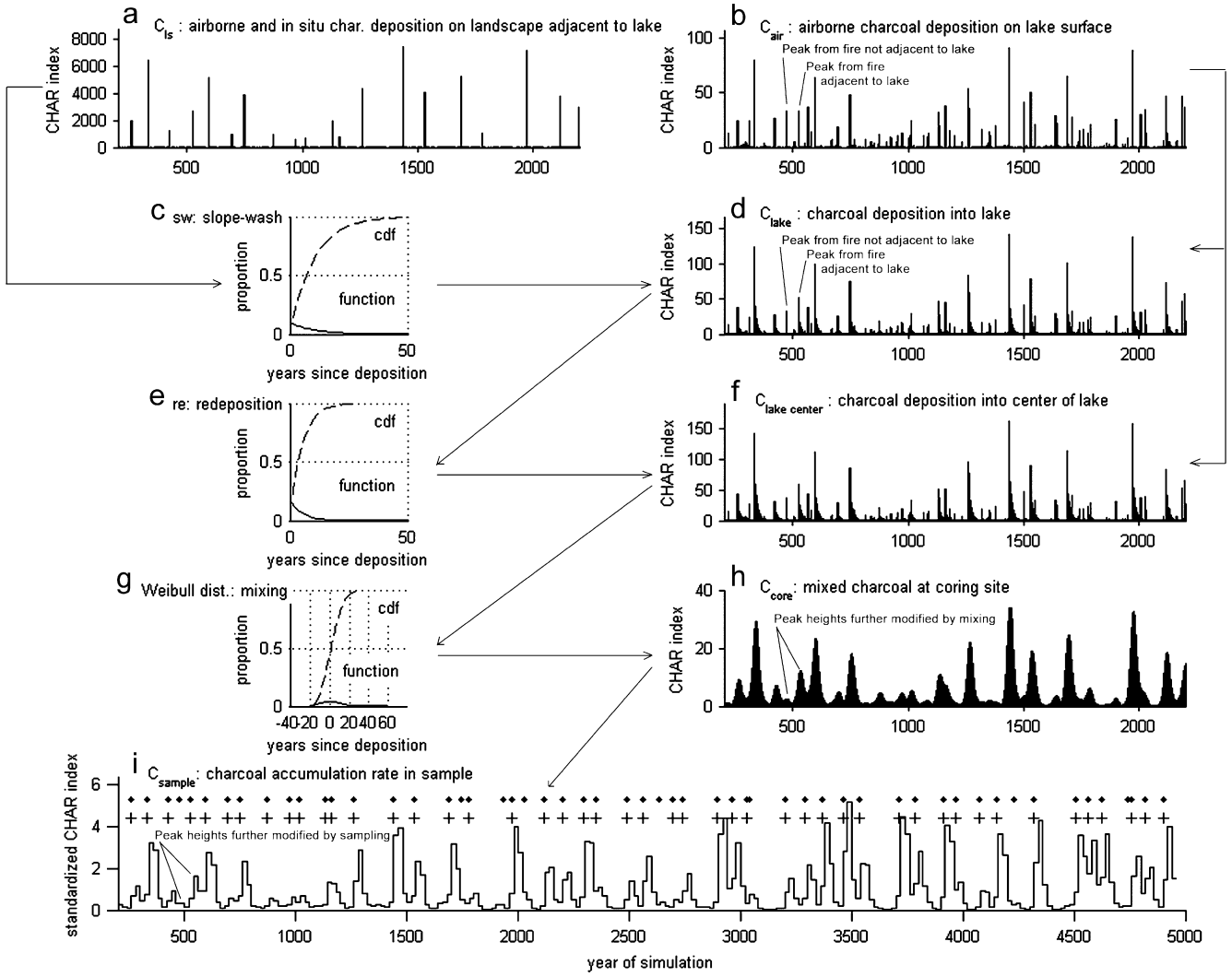

Fig. 1. Charcoal records can be understood largely by visualizing the pathway of charcoal from airborne deposition at and around a lake to its inclusion in a single sediment sample. These processes, as represented in CharSim, are illustrated here for the 1000-m modal injection height scenario and parameters described in Table 2. One percent of the charcoal deposited on the landscape surrounding the lake (C_{ls}; panel a) is distributed into the lake based on the slope-wash curve (sw; panel c). Airborne charcoal deposited on the lake (C_{air}; panel b) is added to charcoal input from slope wash to determine the amount of charcoal deposited on the lake sediment surface (C_{lake}; panel d). One percent of the charcoal on the lake sediment surface is redeposited into the "center" of the lake (defined in Section 2.1.3) based on the redeposition curve (re; panel e) to determine the amount of charcoal reaching the center of the lake (C_{lake_center}; panel f). Charcoal in the center of the lake is mixed according to a Weibull distribution (with shape parameter = 2.5, panel g) to determine the final charcoal stratigraphy within the core (C_{core}; panel h). Finally, the simulated core is sectioned by depth to obtain the sampled values (C_{sample}; panel i). Dots (.) and plus marks (+) indicate when fires burned within 1000 and 100 m of the lake, respectively. Slope wash, mixing, and sampling all magnify the size a charcoal peak originating from a fire adjacent to the lake, as compared to a charcoal peak originating from a fire not adjacent to the lake (panels a, b, h, and i).

shape,[3] excluding any areas that have burned within 50 years (representing low flammability of early successional stands due to limited fuels) until they reach their size, FS_i. Fires start in the study area but grow outside it as necessary.

[3]While real fires grow in complex shapes, often ellipses in boreal forests, in the absence of variability in topography, landform, or inter-fire wind directions, justifying complex fire shapes was deemed arbitrary. Nonetheless, we ran simulations where fire growth favored one cardinal direction, and our results and conclusions did not differ from those reported here.

2.1.2. Primary charcoal deposition

For each year, T, burned pixels contribute airborne charcoal, C_{air}, to the lake and to the eight pixels immediately surrounding the lake based on a charcoal dispersal table (Fig. 2). Charcoal abundance is represented as a proportion, relative to the total amount of charcoal from all burned pixels. A charcoal dispersal table indicates the quantity of charcoal deposited at one pixel (e.g. the lake or pixel adjacent to the lake) given that another pixel burns. When constructed from the perspective of the lake, the charcoal dispersal table is a visual representation of the total area from which charcoal deposited at the lake

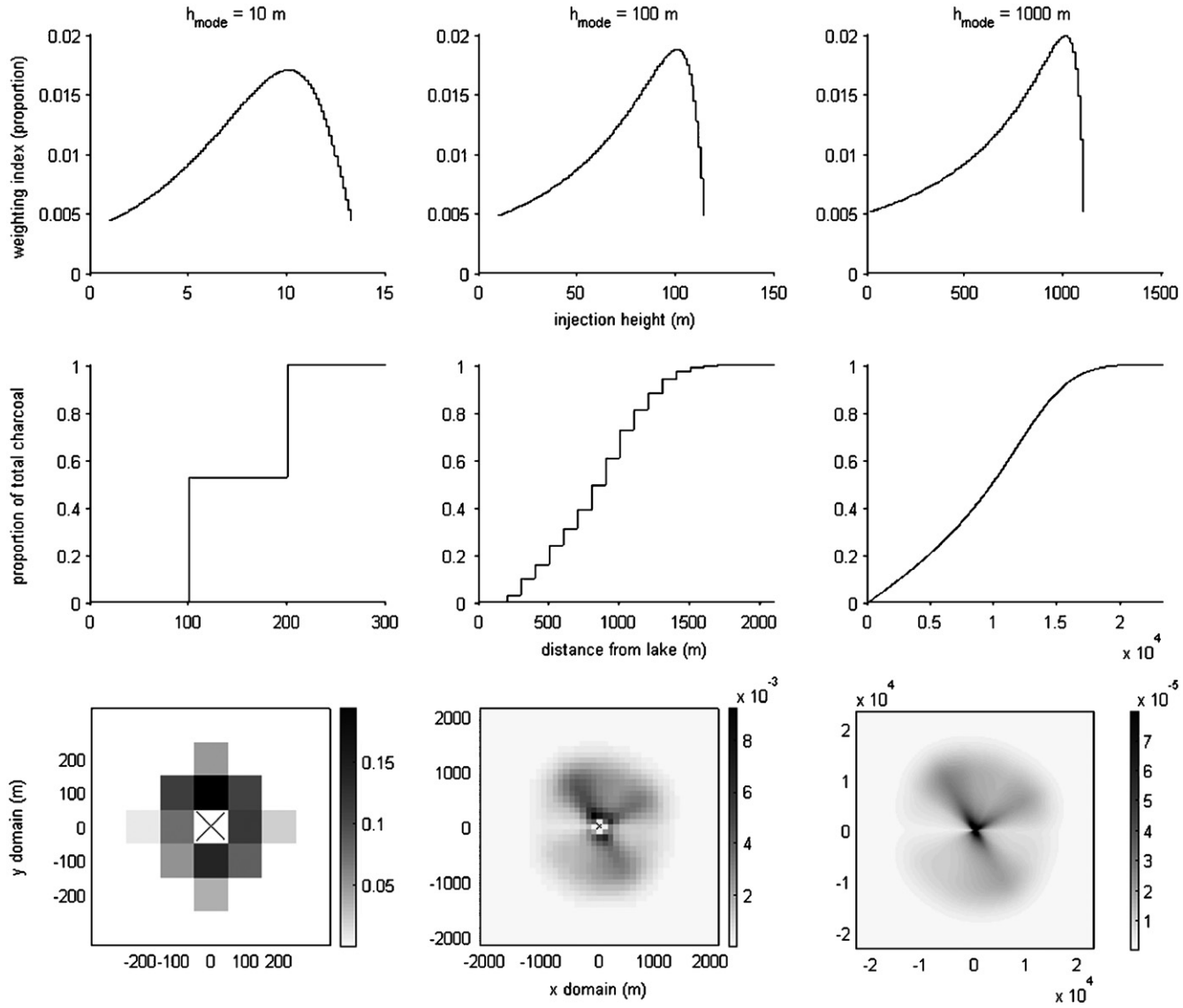

Fig. 2. Development and description of the three charcoal dispersal tables used to simulate charcoal records, identified by their modal injection height, h_{mode} (columns). The entire figure is adapted from Peters and Higuera (2007) to represent the discrete 100×100 m pixel resolution of CharSim. Row 1: distribution of injection heights used to create each dispersal table. Row two: cumulative charcoal deposited at different distances from the lake pixel. The radius of the potential charcoal source area (PCSA) is defined by the distance where 100% of the total charcoal can come from (i.e. 1 on the *y*-axis). In spite of a steep die-off in the amount of charcoal reaching the lake along any one radius, increased area at larger radial distances creates a relatively constant slope, indicating that equal proportions of charcoal *could* come from long distances as from short distances (if the entire source area burned). Row 3: a visual representation of each charcoal dispersal table and PCSA, where different shades of gray (color bars) represent the proportional concentration of charcoal reaching the lake if/when a given pixel burns. Variations in color at a given distance from the lake are a function of the variable wind directions integrated into each dispersal table (see Section 2.1.2, and Fig. 4 in Peters and Higuera, 2007).

originates, termed "the potential charcoal source area" (PCSA; see Peters and Higuera, 2007). Each dispersal table represents the average conditions during a fire that affect the amount of charcoal reaching the lake.

A dispersal table can incorporate any number of assumptions and does not depend on a single dispersal model. A main benefit of using dispersal tables, rather than dispersal curves ("kernels"), is their modularity. Tables can be modified to reflect future knowledge or different assumption and easily substituted within CharSim for existing ones. In addition, dispersal tables insulate CharSim from the assumptions used to make the tables, since CharSim depends only on the table itself. In fact, the behavior of CharSim can be understood to a large extent based simply on the table (i.e. the size and shape of the source area) without knowledge of the dispersal model.

Charcoal dispersal tables were calculated based on a Gaussian dispersal model developed by Sutton (1947), modified by Chamberlain (1953), and applied to charcoal analysis by Clark (1988). In previous work, we modified the model to a two-dimensional form and expanded it to simulate multiple injection heights (the height at which charcoal is released from a buoyant plume) and multiple wind directions (Peters and Higuera, 2007).

Dispersal distances in the modified model are a function of a single fall speed, a single wind speed, and an empirical or theoretical PDF of wind direction and injection heights. We constrained fall speeds to the average fall speed measured in the International Crown Fire Modeling Experiment (ICFME) experimental burn in boreal Canada ($1.56\,m\,s^{-1}$ for particles not passing through a 180 μm sieve; Lynch et al., 2004a; Peters and Higuera, 2007), and we constrained wind speed to the highest 10-m wind speeds measured during several fires from the ICFME ($10\,m\,s^{-1}$, Taylor et al., 2004). Although it may be unrealistic to use a single wind speed and fall speed to represent average conditions during burning, the dispersal model is relatively insensitive to variations in these parameters (Peters and Higuera, 2007). Injection heights and wind direction are much more critical, and these are simulated by PDFs to provide appropriate variation. To simulate multiple injection heights, we assumed a distribution of injection heights during a single fire that has a negative skewness, with a peak at large injection heights and a long tail at smaller heights (Fig. 2, row 1). In contrast to a situation where all charcoal is injected at a single height, this model produces a dispersal table with a strong local bias in charcoal dispersal and no or minimal skip distance (Fig. 2, rows 2–3). To simulate varying wind directions we created a dispersal table with multiple wind directions and then weighted each direction based on an empirical PDF of June–August wind directions from Bettles, Alaska (representing the study area from where empirical records were collected, Higuera, 2006; Table 1). This produces a circular dispersal table with higher values along dominant wind directions (Fig. 2, row 3). The sensitivity of CharSim to assumptions on injection-height distributions and variability in wind directions is described in Appendix A.

We used four injection-height scenarios, characterized by the modal injection height h_{mode}, which span a range of realistic injection heights from wildland fires (e.g. Clark, 1988; Clark et al., 1998; Samsonov et al., 2005). Each scenario represents a different PCSA. In each of the first three scenarios, a single dispersal table was used, based on a specific h_{mode} of 10, 100, or 1000 m. The 10 m h_{mode} scenario gives two-dimensional results similar to empirical data collected from an experimental fire in boreal Canada by Lynch et al. (Lynch et al., 2004a; Peters and Higuera, 2007), while the 100 m and 1000 m h_{mode} scenarios simulate fires with taller plumes (e.g. from larger and/or more intense fires). The fourth scenario was a mixed scenario representing the assumption that injection heights scale with fire size. In the mixed scenario h_{mode} varied with the log of fire size, with each 20th percentile of the log-transformed fire-size distribution calling on a different injection height and dispersal table. Thus, for the smallest 20% of the fires the modal injection height was 10 m; for the next 20%, 50 m; then 100 m; then 500 m, and for the largest 20%, 1000 m.

With a mode and distribution of injection heights selected, there are two ways to portray the PCSA (Fig. 2). Assuming a fire of infinite size, one can consider charcoal deposition at a lake originating from different distances (i.e. radii), as graphically illustrated by the cumulative proportion of total charcoal deposited at increasingly larger radii (Fig. 2, row 2). The PCSA is associated with the radius at which 100% of charcoal originates. A second, more geographic approach is to map the density of charcoal originating in each part of the PCSA (the charcoal dispersal table, Fig. 2, row 3). This illustrates the two-dimensional variations in charcoal dispersal that result from variations in both injection height and wind directions.

2.1.3. Secondary charcoal deposition

Secondary charcoal deposition comes from (1) charcoal deposited on the landscape immediately adjacent to the lake (i.e. the eight pixels surrounding the lake), introduced via slope-wash processes (via water or wind), and (2) charcoal on the lake sediment surface, which is transported to the "center" of the lake, defined as 10% of the lake area, via within-lake redeposition. Both processes are minimally understood. We simulate these processes with a simple negative exponential die-off curve, which moves a given proportion of charcoal from its source (landscape or lake sediment surface) to its end point (lake or lake center) over a certain time frame.

Limited quantitative data are available for selecting parameters for secondary charcoal processes. We assume only a small proportion of charcoal on the landscape surface is transported into a lake basin by slopewash or otherwise (Clark and Patterson, 1997; Lynch et al., 2004a; Carcaillet et al., 2006) and that these processes last until the re-growth of vegetation within the watershed (Clark, 1988; Whitlock and Millspaugh, 1996; Lynch et al., 2004a). We also assumed that within-lake redeposition focuses charcoal in the center of a basin and that charcoal remains mobile for several decades after a fire (Bradbury, 1996; Whitlock and Millspaugh, 1996). To minimize modeling errors associated with these uncertain processes, we selected secondary transport values that are conservative with respect to the amount of charcoal moved by slope wash and within-lake redeposition. Specifically, slope-wash parameters were set to move 1% of all landscape charcoal into the lake basin, with 90% and 99% of the deposition occurring within 20 and 50 years of airborne charcoal deposition (Table 2; Fig. 1c). Within-lake redeposition parameters were set to move 10% of the charcoal from the outer 90% of the lake-sediment surface to the center of the lake, with 90% and 99% of redeposition occurring within 10 and 20 years, respectively (Table 2; Fig. 1e).

The amount of charcoal deposited on the lake-sediment surface in any year due to slope-wash processes, $C_{sw,T}$, is given by

$$C_{sw,T} = p_{sw} \sum_{t=0}^{N_{sw}} sw_t C_{ls,T-t}, \quad (1)$$

Table 2
Parameters used to generate the CharSim records in this study

CharSim component	Description	Parameter (units)	Value(s) used in this paper	
			Variable fire size	Constant fire size
Fire regime	Probability of fire	λ (fires yr^{-1})	1.00	1.00
	Fire size	Mean fire size (log ha)	6.813	8.971
		Std. dev. fire size (log ha)	2.078	0.00
	Resulting mean fire-return interval[a]	yr	120	100
Charcoal dispersal and primary deposition	Injection heights	h_{mode} (m)	10, 100, 1000, mixed[b]	10, 100, 1000
Secondary charcoal deposition	Slope-wash redeposition	p_{sw} (proportion)	0.01	0.01
		slope-wash time frame, N_{sw} (yr)	100	100
		slope-wash mean, μ_{sw}	10	10
	Within-lake redeposition	p_{re} (proportion)	0.10	0.10
		redep. time frame, N_{re} (yr)	50	50
		redep. mean, μ_{sw}	5	5
		proportion of lake defined as center, α	10	10
Mixing	Mixing depth	md (mm)	10	10
	Sed. acc. rate	s (cm yr^{-1})	0.0125	0.0125
Sampling	Sampling interval	d_{sample} (cm)	0.25	0.25
		temporal res. (yr sample^{-1})	20	20

[a]A "fire" is identified any time area burns within a 100 m radius from the edge of the lake, regardless of the number of ignitions that occurred in a year.
[b]The mixed scenario scaled injection heights proportionally to fire size, using h_{mode} values of 10, 50, 100, 500, and 1000.

where $C_{ls,T-t}$, is the amount of charcoal on the pixels immediately surrounding the lake for each year T–t though T, sw_t describes the negative-exponential PDF with mean μ_{sw} (Fig. 1b, c), and p_{sw} is the proportion of landscape charcoal moved into the lake. Only the most recent N_{sw} years contribute charcoal in this fashion. Charcoal on the pixels surrounding the lake, C_{ls}, originates from airborne charcoal deposition and in situ charcoal production when these pixels burn. Airborne deposition is determined in the same fashion as for primary charcoal deposition on the lake (described above). *In situ* charcoal production is defined to be 10 times greater than the total amount of airborne charcoal produced during a fire. This is consistent with a one- to two-order of magnitude difference between charcoal deposition inside and outside experimental fires in boreal forests (Clark et al., 1998; Ohlson and Tryterud, 2000; Lynch et al., 2004a).

Finally, total charcoal deposition on the lake-sediment surface in year T, $C_{lake,T}$ (Fig. 1d) is the sum of airborne charcoal, C_{air} (i.e. primary deposition) and secondary charcoal deposition, C_{sw}:

$$C_{lake,T} = C_{air,T} + C_{sw,T}. \quad (2)$$

Analogous to (1), total charcoal transport to the center of the lake is

$$C_{lake\_center,T} = \alpha C_{lake,T} + (1-\alpha) p_{re} \sum_{t=0}^{N_{re}} re_t C_{lake,T-t}, \quad (3)$$

where re_t describes the negative-exponential PDF with mean μ_{re} (Table 2; Fig. 1e, f). p_{re} is the proportion of charcoal on the non-center portion of the lake-sediment surface which is later redeposited in the center of the lake. N_{re} is the number of years over which within-lake redeposition occurs, and α is the proportion of lake defined to be the center.

2.1.4. Sediment mixing and sediment sampling

A sediment accumulation rate s determines the depth of sediment represented by each year of the model. Charcoal deposited in the center of the lake in year T, $C_{lake\_center,T}$, is mixed into the surrounding strata between mixing depths md_u and md_l above and below each stratum to define charcoal abundance in the core in year T, $C_{core,\,T}$ (Fig. 1h). The sediment accumulation rate s and mixing depth, md ($= md_u + md_l$), define a mixing time window, $T-t_l \leqslant t \leqslant T+t_u$, over which charcoal deposited at time T is mixed. Charcoal in the simulated core at year T is computed, after the core is "made", by mixing charcoal from sediments above and below the depositional strata in this time window, weighted by a Weibull PDF:

$$C_{core,T} = \sum_{t=T-t_l}^{T+t_u} C_{lake\_center,t} \Psi_{T,t}. \quad (4)$$

Here, $\Psi_{T,t}$ represents the PDF of the Weibull distribution with a shape parameter of 2.5 and mode at T, evaluated at t. This distribution slightly biases mixing towards the uppermost sediments (Fig. 1g).

Charcoal abundance in the simulated core is summed across a given sampling depth, d_{sample}, which is translated into an upper and lower sampling time, st_u and st_l, by dividing by the sediment accumulation rate, s (cm yr^{-1}). The units of charcoal abundance C until this point have been a proportion, which we can convert into a charcoal count, charcoal area or another measure of abundance. In order to directly compare with Alaskan records, we chose to use charcoal counts in this paper, consistent with the assumptions underlying the dispersal tables (see Peters and Higuera, 2007). Charcoal counts in each sample are divided by the volume of the sample, v (cm^3; assuming a 7.5-cm diameter circular core), to calculate charcoal concentration (pieces cm^{-3}). The sediment accumulation rate s (cm yr^{-1}) is multiplied by charcoal concentration to obtain the charcoal accumulation rate (CHAR) for each sample, $C_{sample,i}$ (pieces cm^{-2} yr^{-1}):

$$C_{sample,T} = (s/v_{sample}) \sum_{t=st_l}^{st_u} C_{core,t} \quad (5)$$

Finally, to facilitate comparisons between real and simulated records we standardize charcoal accumulation rates by dividing each value by the mean value for the series. We present this as a unitless CHAR index (Fig. 1i).

We selected mixing and sampling parameters that correspond to recent fire history records from lakes in the southcentral Brooks Range, Alaska (Higuera, 2006). The presence of laminations, other stratigraphic layers >1.0 cm, and charcoal stratigraphy in these records suggest that sediment mixing influences roughly between 0.5 and 2 cm (PEH personal observation); sediment accumulation rates over the past 4500 years range between 0.012 and 0.150 cm yr^{-1}. Sampling distances between 0.25 and 0.50-cm sections yield sample intervals between 2 and 42 years (Higuera, 2006).

2.1.5. Comparing CharSim and Alaskan charcoal records

To evaluate the parameter choices in CharSim, we compared several charcoal records from the southern Brooks Range, Alaska (Ruppert Lake, 67°04′16″ N, 154°14′45″ W; Code Lake, 67°09′29″ N, 151°51′40″ W; Wild Tussock Lake, 67°07′40″ N, 151°22′55″ W; Last Chance Lake, 67°04′45″ N, 150°45′08″ W; unofficial names; Higuera, 2006), to simulated records generated using the four h_{mode} scenarios (Table 3) and parameters described in Table 2. To the extent that simulated records produce variability in charcoal series that is similar to empirical records, the representation of processes in the model represents at least one scenario that could explain the creation of actual charcoal records. To the extent that simulated records differ from real records, CharSim is misrepresenting or missing processes affecting the empirical records. We recognize that different processes could lead to the same pattern, so similarity between simulated and observed records in itself is not a rigorous validation of CharSim. A more robust validation requires studies

Table 3
Parameters describing model scenarios used for comparisons to Alaskan sediment-charcoal records and results from two-sample Kolmogorov–Smirnov (K–S) tests

Comparison lake	Prob. of fire λ (fires yr^{-1})	Local fire frequency Mean fire-return interval[a]	Mixing depth md (mm)	Sed. acc. rate s (cm yr^{-1})	Sampling		K–S test result (p-value)			
					d_{sample} (cm)	Temp. res. (yr sample^{-1})	h_{mode} = 10 m	h_{mode} = 100 m	h_{mode} = 1000 m	h_{mode} = mixed[a]
Ruppert	1.0	120	20	0.0125	0.25	20	0.00	0.01	0.26	0.26
Code	1.0	120	10	0.0125	0.25	20	0.00	0.00	0.34	0.71
Wild Tussock	1.0	120	10	0.0125	0.25	20	0.00	0.01	0.25	0.59
Last Chance	1.0	120	5	0.025	0.50	20	0.00	0.00	0.60	0.77

Only CharSim scenarios including long-distance dispersal (i.e. h_{mode} = 1000 m and mixed) were statically indistinguishable from Alaskan records ($0.25 < p < 0.77$).
[a]See Table 2.

quantifying secondary charcoal transport and comparisons to records with known fire histories at a range of spatial scales.

By comparing a single CharSim record to an empirical record we assume the processes creating the empirical record are stationary in time. We thus restrict our comparisons with Alaskan records to the last 3000–4500 yr, which represents a stationary period in the pollen and charcoal history of each record (Brubaker et al., 1983; Anderson and Brubaker, 1994; Higuera, 2006). We evaluated similarity visually with quantile–quantile plots and statistically using a two-sample Kolmogorov–Smirnov test comparing the cumulative distributions of equally sampled CharSim and Alaskan records (Zar, 1999). Alaskan records were standardized to their mean CHAR and, like CharSim records, are expressed as a CHAR index.

2.2. Inferring different aspects of a fire regime

Modeling sediment charcoal records allows one to ask questions that are otherwise impractical or impossible to address empirically. Using CharSim records we addressed two sets of questions that are relevant to the interpretation of sediment charcoal records: (1) how well does airborne and sampled CHAR (C_{air} and C_{sample}) correlate with area burned at different spatial scales, and (2) how well do identifiable charcoal peaks reflect fire occurrence at different spatial scales? For each question we also evaluated how mixing and sampling intervals modify these relationships to ultimately define our ability to infer area burned and/or fire timing in sampled sediment-charcoal records.

2.2.1. Area burned

In CharSim, the annual accumulation of airborne charcoal in the lake is related to area burned in that year, weighted by some function incorporating the distance between the area burned and the lake. Thus charcoal records should represent a distance-weighted index of area burned. To examine such a relationship, we compared both airborne charcoal accumulation, $C_{air,}$ and sampled charcoal accumulation, C_{sample} (using a sampling interval of 20 yr), to annual area burned at multiple radii from the lake using 20,000-yr records generated from the 10- 100- and 1000-m h_{mode} scenarios (Table 2). We use these scenarios to informally test two hypotheses about the relationship between C_{air} and area burned: (1) for any h_{mode} scenario the correlation between annual area burned and C_{air} is maximized at a radius close to that defining the PCSA for that scenario, and (2) the distance of maximum correlation should vary between scenarios. Because the correlation between C_{sample} and area burned differs depending on both sampling interval and mixing interval, we also examined this correlation for 12 sampling intervals from 1 to 2400 years (0.008–20 fires per sample) and 10 mixing intervals from 1 to 150 mm (0.07–1 fire(s) per mixing interval), using the 1000-m h_{mode} scenario. For each of these 120 comparisons, we recorded the maximum correlation and radius at which the maximum correlation occurred (termed the "optimal spatial scale").

2.2.2. "Local" fire occurrence

An alternative approach for interpreting fire history from sediment-charcoal records is to focus on high-frequency, high-magnitude variations (i.e. charcoal peaks). This widely used approach relies on the decomposition of charcoal series into high- and low-frequency components, termed "peak charcoal" and "background charcoal" in the literature (e.g. Whitlock and Anderson, 2003). Ultimately, decomposition turns a charcoal series into a binary record where each sample is categorized into one of two groups: "fire" or "no fire". We evaluated the ability to reconstruct fire occurrence at a range of spatial scales across a range of sampling intervals by analyzing simulated records using the decomposition approach.

To identify charcoal peaks we used the decomposition method in which a smoothed charcoal series, $C_{background}$, representing low-frequency variability is subtracted from the raw series, C_{sample}, to obtain the residual, or peak charcoal series, C_{peak} (Fig. 3). This approach assumes an additive relationship between peak and background components of a charcoal record (e.g. Clark and Royall, 1996). An analyst must select both a smoothing function to define $C_{background}$ and a threshold value to split the C_{peak} series into "fire" and "non-fire" samples. As each CharSim record is associated with a known fire history, it is possible to objectively select the most accurate threshold to infer fires, defined as the "optimal threshold value" (Fig. 3). Specifically, the optimal threshold is the threshold value that maximizes accuracy, defined as the proportion of true positive peaks (peaks correctly identified as fires) minus the proportion of false-positive peaks (peaks incorrectly identified as fires; see Higuera et al., 2005). Furthermore, this measure of accuracy may be calculated for fires within different radii from the lake. We can thus identify the radius at which the charcoal peaks most accurately represent the fire history (i.e. the optimal spatial scale) by finding the radius where accuracy is maximized.

Using this method to identify charcoal peaks, we evaluated the relationship between (1) sampling interval, (2) smoothing interval, (3) maximum accuracy, and (4) the optimal spatial scale of a record. Starting from a single 20,000-year record of airborne charcoal deposition from the 1000-m h_{mode} scenario, we created six records of sampled charcoal using sampling intervals from 2 to 60 years (0.015–0.48 fires per sample) and a mixing interval equivalent to 30 years (0.25 fires per mixing-interval), with parameters otherwise described in Table 2. Each of these six records was decomposed using six different smoothing functions (locally weighted regression robust to outliers (Cleveland, 1979)). These functions varied in length from 0 years (i.e. no smoothing done) to 1200 years (10 fires per smoothing-window). For each of the 36 total records we recorded the accuracy and the optimal spatial scale, representing the best possible interpretation of the record. To test the sensitivity of these results to our assumptions on secondary charcoal transport, we performed the same

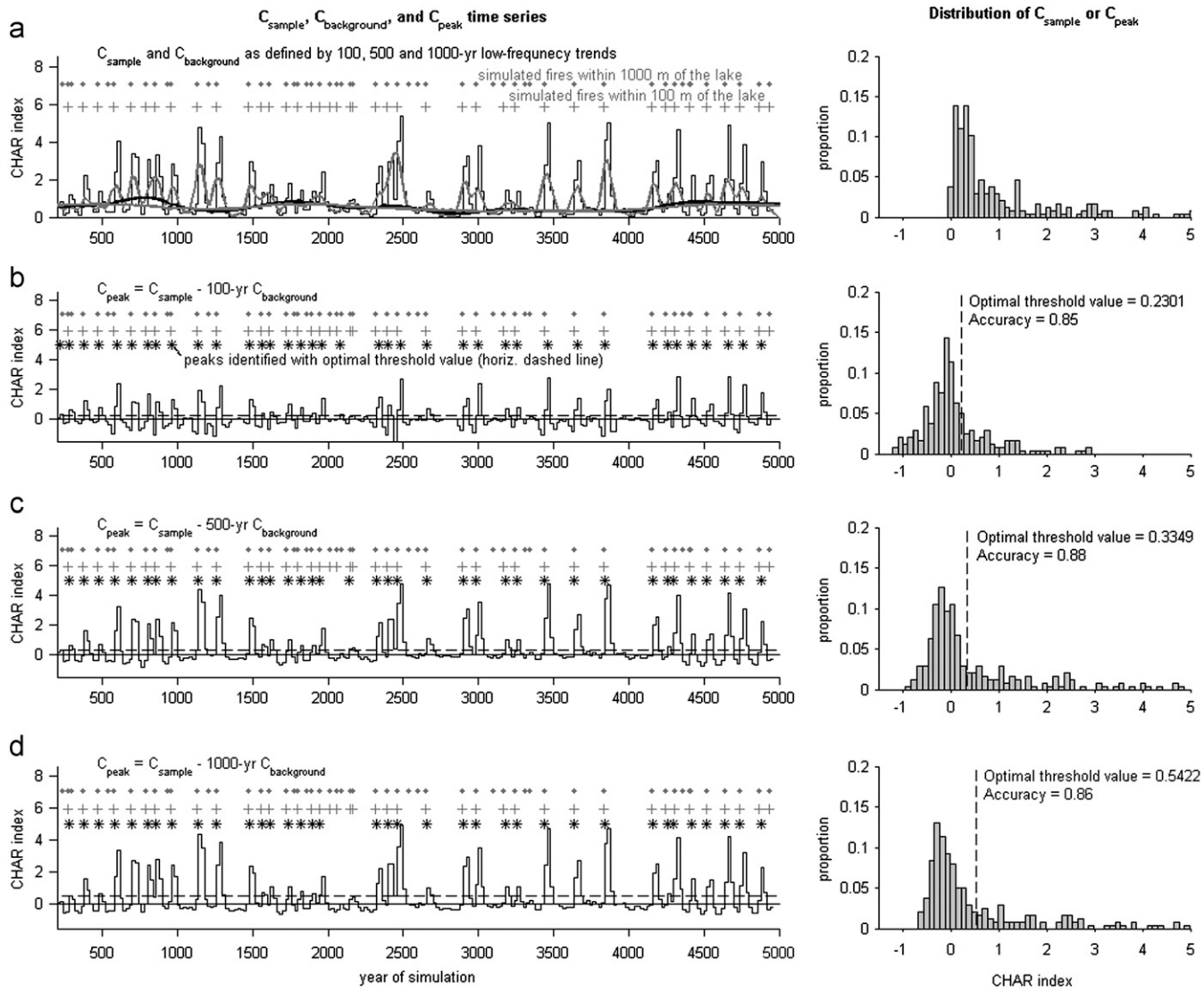

Fig. 3. Contrasting examples of "peak charcoal" records, C_{peak}, used to identify charcoal peaks via decomposition, including the time series (column 1) and frequency distribution (column 2) of each record. Dots (.) and plus marks (+) in column 1 indicate when simulated fires burned within 1000 and 100 m of the lake, respectively. (a) The sampled charcoal record, C_{sample}, with three definitions of "background charcoal", $C_{background}$, based on 100-yr (gray line), 500-yr (black line), and 1000-yr (gray line) trends in C_{sample}, defined with a locally weighted regression robust to outliers (Cleveland, 1979). (b)–(d) C_{peak} series have background trends subtracted and thus include both positive and negative CHAR index values. When C_{peak} values exceed a globally applied threshold, peaks are identified and fires inferred (*symbols). The optimal threshold value for each record, maximizing the accuracy of fire history interpretations (see Section 2.2.2), is indicated by the horizontal dashed line in column 1 and the vertical dashed line in column 2. In this example, 42 fires burned within 100 m of the lake (the "+" ca yr 1500 represents two fires) and in all cases (b–d) the most accurate interpretation of fire history is obtained by comparing charcoal peaks to fires within 100 m of the lake (i.e. the optimal spatial domain = 100 m). Removing 500-yr trends from the raw record (panel c) yields the highest accuracy by detecting 37 of 42 fires (88%) and having 0 false positives. The other two options have lower accuracy, either because of false positives (panel b; 1 of 38 peaks, 3%) or fewer fires detected (panel d; 36 of 42 fires, 83%).

simulations with secondary charcoal transport eliminated (i.e. $P_{sw} = P_{re} = 0$).

3. Results

3.1. Charsim simulations: sources of variation and sensitivity

3.1.1. Parameters controlling primary charcoal deposition

The variability in peak heights in CharSim records is most sensitive to the size of the PCSA relative to the fire size (termed "source-area to fire-size ratio"): if the source-area to fire-size ratio is large, peak heights vary broadly, while if the source-area to fire-size ratio is small, all peaks are about the same size. Two relationships account for this result. First, if fires frequently cover large portions of the PCSA (i.e. small source-area to fire-size ratio), the resulting record of charcoal accumulation is approximately binary. This is the case for the 100-m (Fig. 4a) and 10-m (not shown) h_{mode} scenarios. However, with the same fire size distribution and increasing PCSA (1000-m h_{mode} scenario; Fig. 4b), smaller portions of the source area burn in any

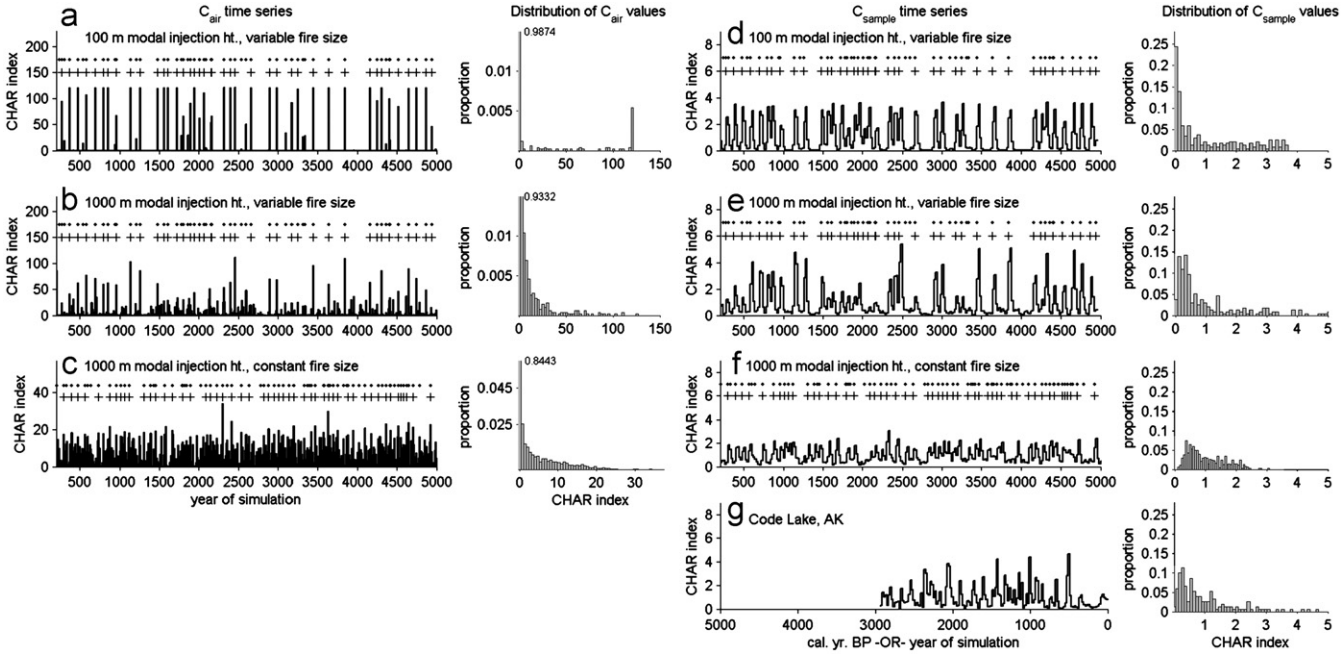

Fig. 4. Examples illustrating that the variability in charcoal peak heights in simulated records results from (1) larger modal injection heights, h_{mode}, (2) variability in fire size, and (3) the inclusion of secondary charcoal transport, mixing, and sampling. (a) 100-m h_{mode} scenario with variable fire sizes produces binary charcoal distributions significantly different from observed records from Alaskan lakes (g, Fig. 5). (b) Increasing injection heights to those characterized by 1000-m h_{mode} scenario increases variability in charcoal peak heights. (c) Keeping large injection heights (i.e. 1000-m h_{mode} scenario) but eliminating variability in fire size produces homogenous records with a narrow range of CHARs (i.e. b vs. c; note factor of four difference in the CHAR index). (d)–(f) Mixing and sampling homogenize records and produce more continuous CHAR distributions. (g) Only the mixed and sample record from the 1000-m h_{mode} scenario is similar to Alaskan records.

single fire. Thus the greater variability in fire location within the source area creates variability in charcoal peak heights. Second, the variability in fire sizes within the PCSA causes variability in simulated charcoal records. For example, if the distribution of fire sizes from the Alaskan database is replaced with a uniform distribution such that the total area burned remains relatively constant (Table 2), the variability in charcoal peak heights decreases by roughly a factor of four (Fig 4c) for the 1000-m h_{mode} scenario. In contrast, variability in wind direction, as modeled here, has only minor effects on the variation in charcoal accumulation (Appendix A).

3.1.2. Parameters controlling secondary charcoal deposition

In the scenarios, the transport of 1% of landscape charcoal from fires burning adjacent to the lake had a minor but visible impact on peak heights (Fig. 1b vs. d). In addition to modifying peak heights, slope-wash added charcoal to sediments in years after primary charcoal deposition (Fig. 1d). Within-lake redeposition also distributed charcoal to years following primary deposition, but this process did not affect relative peak heights (Fig. 1d, f).

3.1.3. Parameters controlling sediment mixing and sampling

Sediment mixing and sampling had large impacts on the patterns of airborne charcoal deposition. Because these processes act on all charcoal within any given stratigraphic level, they spread charcoal out across multiple years of sediment accumulation (in this case approximately 20), thereby modifying peak heights (as much as a factor of four), combining adjacent peaks, and erasing small peaks (e.g. Fig. 1b-f vs. h, i). Below, we analyze the relationship between mixing and sampling intervals and how the choice of sampling interval affects our interpretation of sediment records.

3.2. Comparing CharSim and Alaskan charcoal records

Only the 1000-m and mixed h_{mode} scenarios (charcoal dispersal distances up to ca 20 km) captured the variation of charcoal accumulation in the Alaskan records, with the mixed scenarios generally providing closer fits to empirical data (Table 3). The variability in peak magnitude within the Alaskan records, particularly at CHAR index values >2, was least well represented in the simulated records (Fig. 5). For example, the poorest fit between Alaskan and CharSim records was from Ruppert Lake (Table 3), which contains two peaks 1.5 and 2 times larger than the largest peaks in the CharSim record (Fig. 5). The 10- and 100-m h_{mode} scenarios, with charcoal dispersal distances of approximately 0.25 and 2 km, respectively (Fig. 2), created nearly binary records with variations unlike the Alaskan records (Fig. 4).

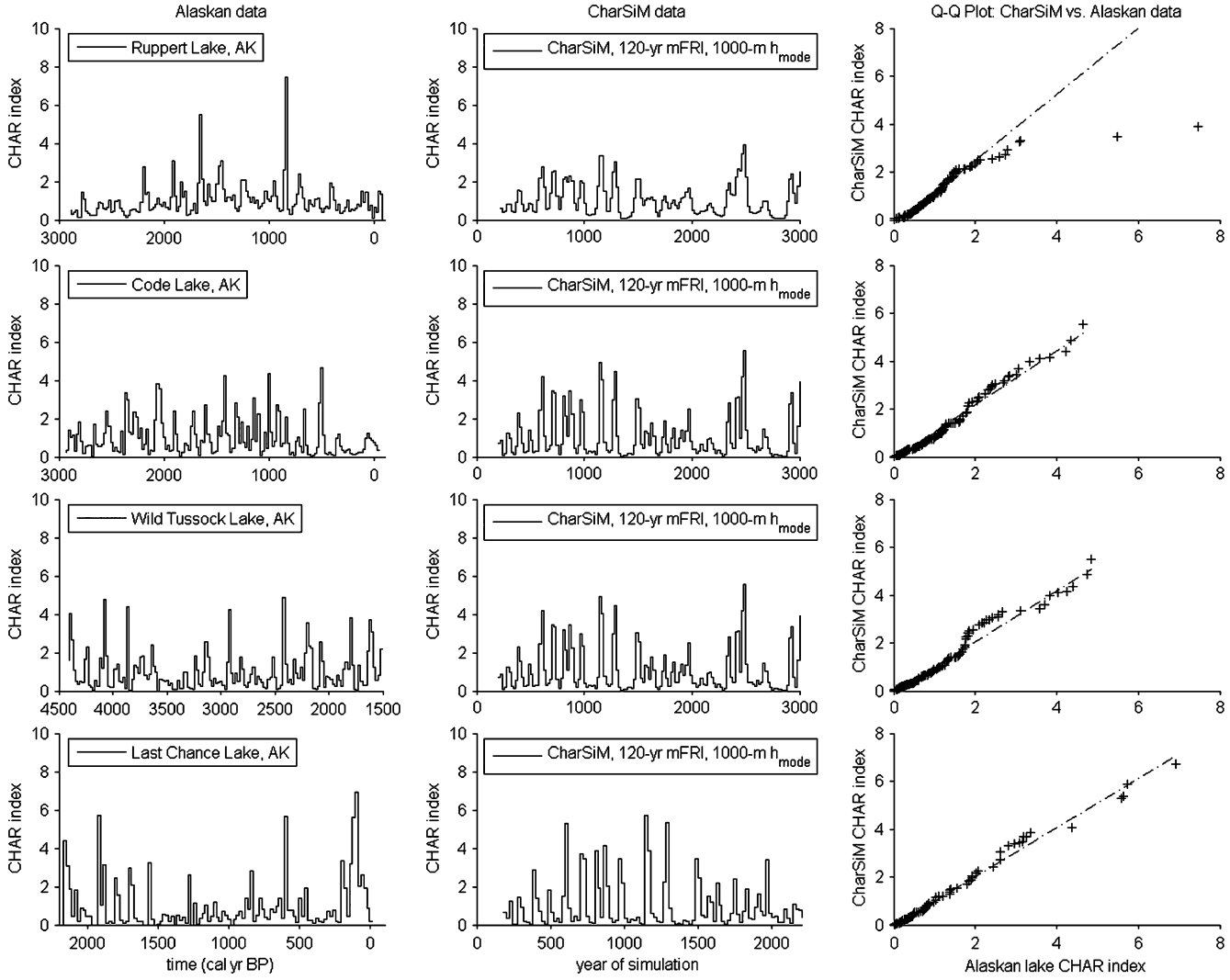

Fig. 5. Charcoal accumulation rates from Alaskan lakes are similar to simulated CharSim records using the 1000-m modal injection height scenario (columns 1–2). Linear quantile–quantile (Q–Q) plots (column three) suggest that empirical and simulated records come from the same distribution, and a two-sample Kolmogorov–Smirnov test comparing the empirical and simulated distributions fails to reject the null hypothesis of no difference ($p \geqslant 0.25$; Table 3). In all cases the Q–Q plots depart from linearity at CHAR index values >2, indicating that the variability in the magnitude of large peaks is least well represented in the CharSim records.

3.3. Inferring different aspects of a fire regime

3.3.1. Area burned

Airborne charcoal accumulation C_{air} and annual area burned within a given radius are significantly correlated ($p < 0.05$, $r^2 > 0.90$) at radii close to the radius defining of the PCSA (ca $10 \times h_{mode}$; Fig. 6, filled symbols). In comparison, the correlations between sampled charcoal accumulation C_{sample} and area burned were much lower ($r^2 < 0.50$) and less sensitive to different radii (Fig. 6, open symbols).

Correlations between C_{sample} and area burned increased with sampling intervals, reaching a maximum of 0.80 when sampling intervals included an average of 11 fires per sample (i.e. the sampling interval was 11 times the mean fire return interval [mFRI; 120 yr, Table 2]; Fig. 7). Optimal spatial scales at these sampling intervals approached the scale defined by the PCSA and were either 16,000 m ($n = 49$; 45%) or 8,000 m ($n = 61$; 55%). Correlations between C_{sample} and area burned were also affected by mixing, but primarily at small sampling intervals (Fig. 7).

3.3.2. "Local" fire occurrence

For a given mixing rate, the accuracy of identifying local fire occurrence is a function of the spatial scale of the record, the smoothing window, and the sampling resolution relative to the mFRI. Maximum accuracy occurred when sampling intervals were <0.12 times the mFRI (e.g. 12 yr for a 100 yr mFRI) and was sensitive to the smoothing windows at these intervals. Optimal smoothing windows were generally 2–5 times the mFRI (Fig. 8), which

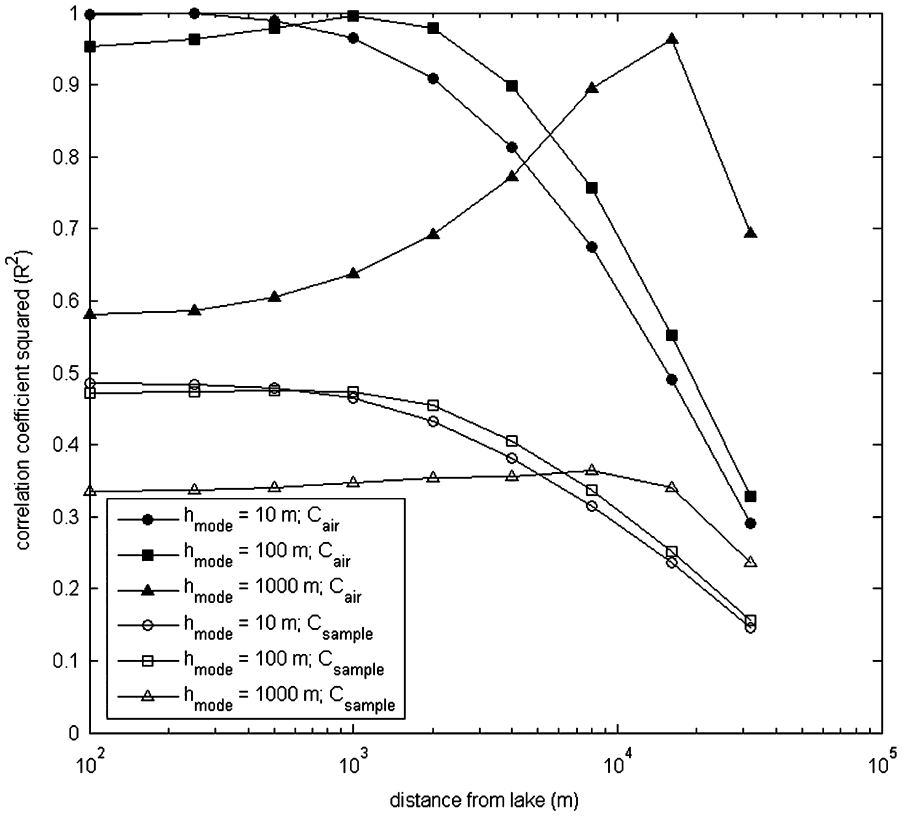

Fig. 6. The correlation (y-axis) between airborne charcoal accumulation (C_{air}, filled symbols) and area burned, and between sampled charcoal accumulation (C_{sample}, open symbols) and area burned varies with distance from the lake (x-axis) and for each dispersal scenario (h_{mode} = 10, 100, and 1000 m). For airborne charcoal, correlations with area burned approach 1 at the distance defining the potential charcoal source area (PCSA) while correlations decrees at both shorter and longer distances. The high correlations between C_{air} and area burned are greatly reduced when secondary processes (e.g. mixing and sampling) are included in the C_{sample} records. The variation in correlation coefficients at different distances is also reduced in the C_{sample} relative to C_{air} records. Resolution in sampled scenarios is 20 yr per sample.

is shorter than the smoothing window maximizing the correlation between sampled charcoal C_{sample} and area burned. At larger sampling intervals, accuracy was less sensitive to smoothing windows, although smoothing windows shorter than the mFRI were associated with low accuracy (Fig. 8). Very long smoothing windows failed to remove short-term variations associated with secondary transport and mixing, resulting in reduced accuracy due to false-positives. Short smoothing windows tracked peak heights too closely and resulted in reduced accuracy because of lowered true-positive rates (e.g. Fig. 3).

The maximum accuracy of fire identification occurred at much smaller spatial scales than those maximizing the correlation between C_{air} and area burned. Of the 36 records analyzed for accuracy, the optimal spatial scale was defined by a 100 m ($n = 35$) or 200 m ($n = 1$) radius (data not presented graphically). When secondary charcoal transport was eliminated (i.e. $P_{sw} = P_{re} = 0$), optimal spatial scales were defined by only slightly larger radii, at 100 m ($n = 16$; 44%), 200 m ($n = 19$; 53%) or 500 m ($n = 1$; 3%; data not presented graphically). Accuracy in all scenarios was less than 0.85 and limited by lower true-positive rates rather than by higher false-positive rates. For example, while no false positives occurred at the optimal threshold values, sediment mixing combined peaks from fires closely spaced in time (e.g. <20 yr, Fig. 3) so that some fires were not detected.

4. Discussion

4.1. Assessment of CharSim

The simulation results show that the random placement of realistically sized fires on a homogenous landscape and a few basic assumptions about charcoal dispersal and taphonomy create charcoal records consistent with Alaskan sediment records. Nevertheless, CharSim is limited by a lack of empirical data and an incomplete understanding of key processes. Therefore, we place our interpretations within several constraints. First, although charcoal dispersal is simulated with a physically based dispersal model that successfully reproduces data from an experimental fire (Peters and Higuera, 2007), we lack a strong empirical or theoretical basis for choosing the distributions of injection heights, and our model does not incorporate topographic variability common to mountainous terrain. Given the simplicity and hypothetical nature of the dispersal scenarios, the dispersal distances, PCSAs, and optimal spatial

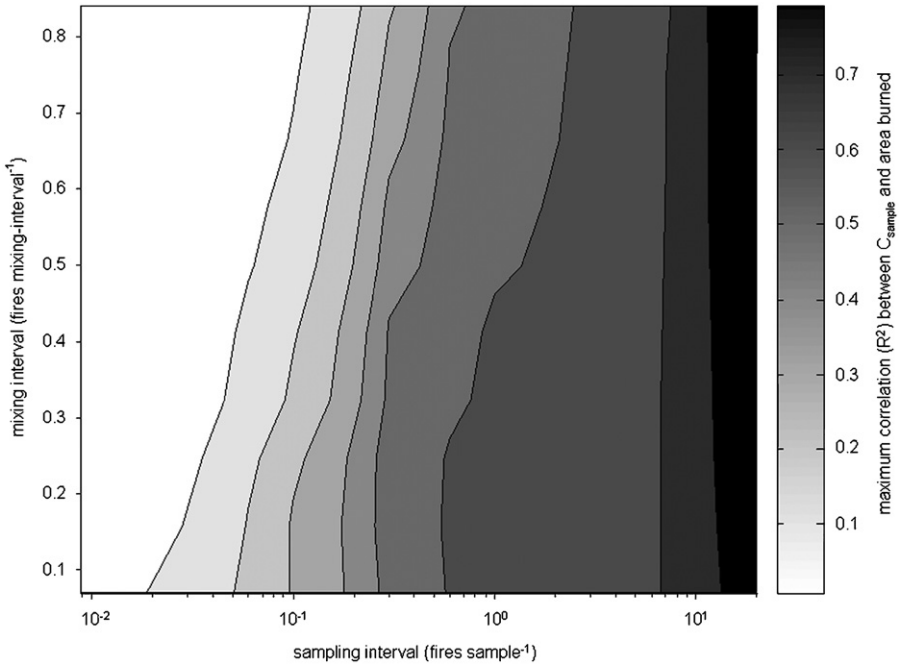

Fig. 7. The maximum correlation between sampled charcoal accumulation, C_{sample}, and area burned (z dimension, color bar) increases primarily as sampling intervals (x-axis) increase and secondarily as mixing intervals (y-axis) decrease. When C_{sample} records are sampled at large intervals (e.g. 10 fires per sample, or 1000 years for a system with a 100 yr mFRI), correlations between sampled charcoal accumulation and area burned within 8–16 km (see below) approach 0.80. This is analogous to smoothing a finely sampled charcoal record to obtain a long-term average (i.e. "background"). Correlations are based on 10 mixing and 12 sampling intervals, standardized to the mean fire return interval (120 yr), from a 20,000-yr record using the 1000-m h_{mode} scenario and parameters described in Table 2. Correlations from all radii in Fig. 6 were considered, but only the maximum correlation is graphed. Optimal radii were either 8 or 16 km, with and average of 11 km (std. dev. 4 km).

scales should be interpreted as first-order estimates for topographically simple landscapes. Despite these cautions, the general conclusions about the relative roles of PCSA and fire size are robust to a variety of assumptions concerning the form of the distribution of injection heights and wind direction (Appendix A). Second, we know little about the rates and variability of charcoal input via slope wash and redeposition. While the simulations address the role of these secondary transport processes, our inferences rely on minimally constrained assumptions. For example, we did not model scenarios in which the variability of secondary charcoal input was high enough to create variability in simulated records similar to that observed in airborne charcoal deposition. While possible, this scenario seems unlikely because it requires extremely high, short-term variations in processes delivering secondary charcoal to sampling sites. Such questions highlight the need for additional research on the effects of secondary charcoal transport. Third, we do not simulate variable sediment accumulation rates or mixing depths. Non-stationarity in these processes may account for the different magnitudes of the largest charcoal peaks in simulated vs. empirical records (Fig. 5). Finally, we have not addressed the effect of lake size, which is an important variable for understanding modeled and empirical pollen data (e.g. Sugita, 1993). We do not expect substantial differences in charcoal peak heights as a result of moderate increases in lake size (e.g. from 1 to 10 ha), so long as lake size remains small relative to fire sizes and the PCSA (as in the scenarios creating realistic simulated records). For a given PCSA, if lake size approaches fire sizes, then variability in airborne charcoal deposition and the overall variability in the charcoal record should be reduced. This may affect the optimum spatial scale of inference using the decomposition method. Future development of CharSim will help test these and other hypotheses about the effects of lake size.

4.2. Processes creating variability in sediment charcoal records

4.2.1. Primary charcoal deposition

At the most fundamental level, the amount of primary charcoal deposited in a lake is a function of the size and location of burned areas within the PCSA. If the PCSA captures only a small portion of the variability in fire size and location, airborne charcoal deposition will vary little between fire events. This is the case in the small PCSA scenarios ($h_{mode} = 10$ and 100 m; ~0.2 and 13 km^2, respectively), which show little variation in charcoal deposition among fires because most fires either cover the entire PCSA or miss it completely. In these scenarios, airborne charcoal deposition creates a nearly binary pattern of charcoal accumulation through time (Fig. 4a). However, as PCSA size increases ($h_{mode} = 1000$ m; 1300 km^2), variability in primary charcoal deposition

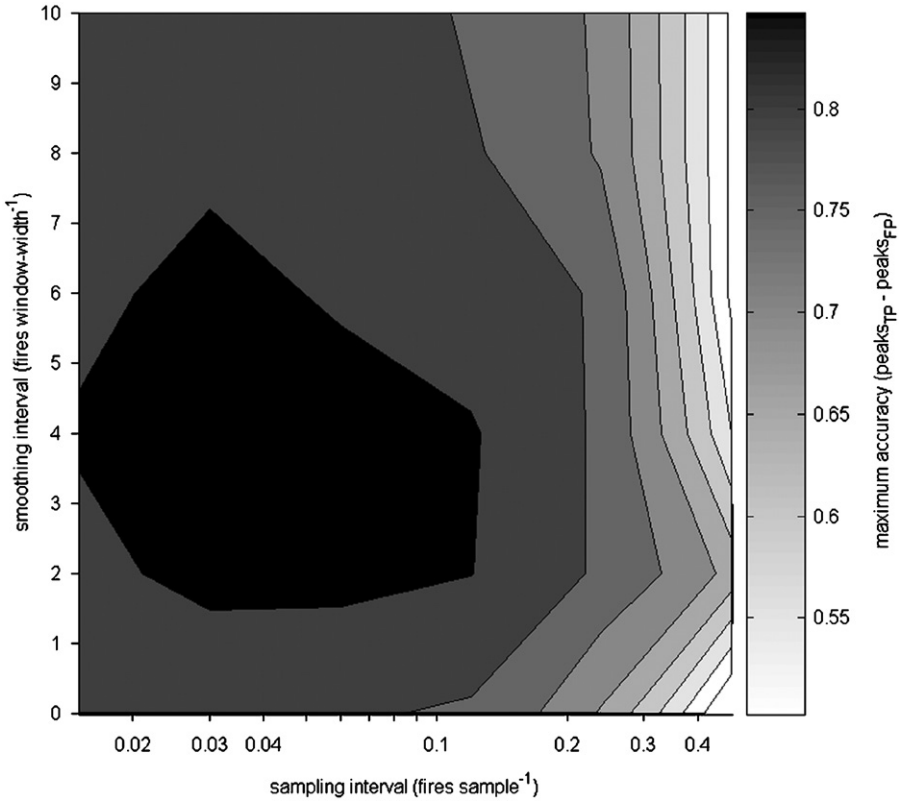

Fig. 8. When analyzing simulated records using the decomposition approach, maximum accuracy (z-dimension, color bar) was obtained from records with small sampling intervals (x-axis) and when intermediate smoothing intervals (y-axis) were used for decomposition. Accuracy values are based on 6 different sampling intervals and 6 different smoothing intervals, normalized to the mean fire return interval (120 yr), from the same base record used for Fig 6. Mixing is equivalent to 0.3 (fires mixing-interval^{-1}) in Fig. 7, and a smoothing interval of zero corresponds to analyzing the raw record (i.e. no trends removed). Accuracy values range from 0.50 to 0.85 and were maximized at spatial domains defined by a 100-m or 200-m radius from the lake (see results).

increases because there is greater variability in the locations and sizes of fires within the source area.

Because the fire sizes in CharSim are well constrained by the Alaskan fire database, the results allow inferences about charcoal source areas in boreal forests of this region. In particular, the correspondence between CharSim simulations and empirical records (Fig. 5, Table 3) suggests that charcoal dispersal distances exceed 10 km (source areas $>300\,km^2$). This finding contrasts with evidence from experimental fires in boreal forests (Clark et al., 1998; Ohlson and Tryterud, 2000; Lynch et al., 2004a) suggesting that macroscopic charcoal travels much shorter distances (e.g. 10's–100's of meter; source areas $<3\,km^2$). When CharSim simulations are based on these smaller dispersal distances (10- and 100-m h_{mode} scenarios), unrealistic binary charcoal records are produced that contain distinct peaks and little charcoal otherwise (e.g. Fig. 4a, e). These results support the pattern predicted by Peters and Higuera (2007) based solely on examining the dispersal tables used in this study. High-magnitude, short-term variations in secondary charcoal delivery is a possible mechanism through which a simple, binary record could be modified, but this scenario seems unlikely for the reasons discussed above (see "Assessment of CharSim"). The larger charcoal dispersal distances suggested by CharSim are consistent with studies documenting charcoal deposition (Pisaric, 2002; Tinner et al., 2006) or charcoal peaks in lakes that are several kilometers away from wildfires (e.g. Whitlock and Millspaugh, 1996; Gardner and Whitlock, 2001; Hallett et al., 2003). Furthermore, the large injection heights (e.g. up to 1000 m) required to simulate large charcoal source areas are tenable given plume heights of 2000–5000 m in observed wildfires (Clark et al., 1998; Samsonov et al., 2005).

4.2.2. *Secondary charcoal deposition, sediment mixing, and sediment sampling*

Secondary transport, mixing, and sampling have variable effects on sediment charcoal records. These processes confound the relationship between primary deposition and annual area burned because they erase or combine small, closely spaced peaks by spreading charcoal across time periods before and after primary charcoal input. Although in the simulations none of these processes (alone or in combination) could create the variability seen in the Alaskan sediment records, they were necessary to produce records that visually resemble empirical records (e.g. Fig. 2b vs. g). Thus one interpretation suggested by CharSim simulations

is that the variability in charcoal records originates through mechanisms controlling primary deposition, and taphonomic processes and sampling intervals temporally smooth these series. On the other hand, the simulations also show that secondary transport can add variability to charcoal peaks that is unrelated to primary input. This occurs when slopewash from burned pixels immediately surrounding the lake (even at minimal rates of 1% per 50 years) increases the size of charcoal peaks relative to peaks created from more distant fires (Fig. 2a vs. b). This effect is subtle and is a consequence of the assumption that charcoal deposition within a fire is 10 times greater than charcoal deposition beyond a burned area (Clark et al., 1998; Ohlson and Tryterud, 2000; Lynch et al., 2004a). Thus abundant charcoal on a burned landscape represents a potentially important source of charcoal input to sediment records, and erosional inputs from the surrounding landscape could magnify the local bias of sediment charcoal records (Clark and Patterson, 1997).

4.3. Methodological implications: analyzing sediment charcoal records via decomposition

Given the known fire history creating each simulated charcoal record, simulated records provide an opportunity to examine assumptions and interpretations of the decomposition approach to sediment-charcoal analysis. The correlation between low-frequency trends in charcoal accumulation and area burned within relatively long distances from the lake (e.g. >5 km) provides support for previous interpretations of background charcoal. Results also indicate that charcoal records can be analyzed in a manner that faithfully represents "local" fire occurrence. Overall, the results lend theoretical support to two main assumptions of sediment charcoal analysis (e.g. Clark and Royall, 1996; Clark and Patterson, 1997; Long et al., 1998): that charcoal records contain (1) low-frequency (long term) trends reflecting area burned at large spatial scales and (2) high-frequency (short term) variations that reflect fire occurrence at small spatial scales.

4.3.1. Area burned

The result that low-frequency summaries ($>10\times$ the mFRI) of charcoal records can accurately reflect area burned within the PCSA (Fig. 7) is consistent with the original concept of "background" charcoal (Clark and Royall, 1995b; Clark and Royall, 1996; Clark et al., 1996; Clark and Patterson, 1997). While airborne charcoal deposition at a lake can be highly correlated with area burned in annual times scales (Fig. 6), secondary transport, mixing, and sampling, distribute annual charcoal deposition over longer time periods in sediments, resulting in poor short-term, but strong long-term correlations between sampled charcoal and area burned (Fig. 7). If secondary transport, mixing and/or sampling vary at shorter time scales than the smoothing window used to define "background" charcoal, then long-term summaries of charcoal accumulation should be accurate descriptions of area burned, although inherently with low temporal resolution. However, the relationship between "background" charcoal and area burned assumes that the amount of charcoal produced per unit area burned and secondary deposition rates remain relatively constant. If charcoal production increased (e.g. from changing vegetation type, Marlon et al., 2006) or secondary deposition increased (e.g. from changing sedimentation regimes, Long et al., 1998), there would be an overall increase in charcoal accumulation, even if fire frequency or sizes did not change. In general, though, the interpretation of low-frequency trends in charcoal accumulation is a potentially valuable way to infer regional burning patterns over multi-centennial to multi-millennial time scales.

4.3.2. "Local" fire occurrence

Our results suggest that the optimal sampling interval for detecting individual fires is <0.12 times the mFRI (Fig. 8), with the ability to detect fires decreasing quickly at larger intervals because charcoal peaks from distinct fires are combined. This finding is similar to conclusions of Clark (1988), who recommended sampling intervals <0.2 times the return interval of interest, based on visual analysis of charcoal peaks in simple simulated records with different sampling intervals.

We found that charcoal peak identification in simulated records most accurately reflects fire occurrence within 500 m of the lake (Fig. 8). This result is consistent with Gavin et al.'s (2003) finding that the maximum correspondence (i.e. accuracy) between charcoal peaks and fires occurred when fires burned within 500 m of a lake on Vancouver Island, Canada. More generally, the results imply that long-distance charcoal transport does not preclude the accurate detection of local fires. For example, the PCSA in the 1000-m h_{mode} scenario extends to 20 km from the lake, yet charcoal peaks most accurately reflect fires within 500 m. What then explains the bias of charcoal peaks to local fires? First, the distance weighting inherent in charcoal dispersal results in local fires always creating larger charcoal peaks than more distant fires. Second, secondary transport, mixing and sampling dampen small charcoal peaks, while large charcoal peaks are robust to these processes. Third, the decomposition approach, which removes low-frequency trends, emphasizes large charcoal peaks and thereby amplifies the inherent biases against small and/or distant fires. However, other decomposition techniques can amplify small peaks, for example when using a threshold ratio and/or transforming a charcoal record. The sensitivity of our results to decomposition choices is beyond the scope of this study but will be the focus of future research utilizing CharSim.

4.3.3. Concepts of "background" and smoothing windows

The concept of "background" charcoal is represented by a low-frequency summary of a charcoal series over some time window, defined by the "smoothing window" (Fig. 3).

This representation of background has been used in two distinct ways in the charcoal literature, each with theoretical justification and support from the CharSim simulations. First, background charcoal has been interpreted to represent area burned at large temporal and spatial scales (Clark and Royall, 1995a; Clark et al., 1996; Clark and Patterson, 1997). This definition of background is justified in CharSim by the high correlation between area burned and charcoal accumulation for sampling intervals $>10\times$ the mFRI. Thus the smoothing window used to depict this definition of background should be greater than $10\times$ the inferred mFRI. Although background charcoal could also reflect changing vegetation types and long-term changes in charcoal delivery mechanisms (e.g. Long et al., 1998; Clark et al., 2001; Marlon et al., 2006), neither was modeled in this study. Second, background charcoal has been associated with a smoothing window that isolates high-frequency variations in CHAR in the decomposition processes (e.g. Clark et al., 1996; Long et al., 1998; Carcaillet et al., 2001a; Lynch et al., 2002; Gavin et al., 2003). The simulations suggest that it is possible to select windows that maximize the accuracy of charcoal-record interpretations when sediments are sampled at fine intervals (e.g. <0.1 times the mFRI) but that accuracy is generally insensitive to smoothing windows when sampling intervals are larger (Fig. 7). Nevertheless, smoothing windows 2–5 times the mFRI resulted in the highest accuracy at all sampling intervals. The smoothing window for decomposition can, therefore, be considered separately from the window used to estimate long-term trends in area burned.

We suggest distinguishing the ecological and functional interpretations of the term "background". Ecologically, background charcoal may represent the total amount of charcoal in a sediment record and be controlled by several processes related to the fire regime. Functionally, the term applies to the analytical goal of removing variations not associated with "local" fire occurrence, which mainly originate from taphonomic processes of mixing and sampling. In this case, we suggest the term "low frequency variation", which emphasizes the physical pattern of charcoal accumulation without implications about fire or ecological processes.

5. Conclusions

Based on empirical data of Alaskan fire regimes and specific assumptions of charcoal transport and taphonomy, CharSim produces charcoal records that resemble sediment-charcoal records from boreal Alaska. In addition, CharSim simulations illustrate several connections between processes that affect sediment charcoal records and the decomposition approach used to interpret fire history from these records.

First, simulations indicate that charcoal records reflect area burned within the PCSA, but that secondary transport, sediment mixing, and sampling dampen this relationship at short time scales (e.g. $<$mFRI). As a result, simulated and empirical (e.g. Enache and Cumming, 2006) records are only moderately correlated with area burned at short time scales, but simulated records are highly correlated with area burned within the PCSA at long time scales ($>10\times$ mFRI). These results lend support to the use large smoothing windows to describe "background" charcoal (as defined above) and infer regional area burned.

Second, the variability in charcoal peak heights in simulated records can largely be explained by relationships between fire sizes and the PCSA size (the source-area to fire-size ratio). As this ratio increases in CharSim simulations, the variability in charcoal peak heights also increases because there is greater variability in fires sizes and locations within the PCSA. Comparisons of simulations with different source-area to fire-size ratios to Alaskan charcoal records suggest that large source areas, characterized by long-distance charcoal transport (10 s of km), are required to obtain the basic patterns of variability in charcoal records from systems with large fire sizes (e.g. boreal forests). These dispersal distances are consistent with evidence of charcoal transport from wildland fires of tens of kilometers (Whitlock and Millspaugh, 1996; Gardner and Whitlock, 2001; Pisaric, 2002; Hallett et al., 2003). However, long-distance transport per se does not erase the strong relationship between large charcoal peaks and local fires. In our simulations inferred fires using the decomposition approach are best related to fire occurrence within 500 m of the simulated lake. Interpreting "local" fires at this spatial scale is consistent with empirical studies comparing known fires to sediment charcoal stratigraphy (Clark, 1990; Whitlock and Millspaugh, 1996; Gavin et al., 2003; Lynch et al., 2004a; Higuera et al., 2005).

Third, the charcoal-taphonomic processes of slope wash, mixing, and sampling bias sediment records against preserving small charcoal peaks associated with small and/or distant fires. By removing low-frequency variations, the decomposition approach further de-emphasizes small peaks. The overall result of the decomposition method, therefore, is to enhance the signature of local fire occurrence, while simultaneously accounting for long-term variability in charcoal accumulation rates.

Acknowledgements

This work was funded by the US National Science Foundation through a Graduate Research Fellowship to PEH and award number 0112586 to LBB, Patricia Anderson, and Thomas Brown from the Arctic System Science Program. We thank Douglas Sprugel for valuable insights throughout this work and for reviewing earlier versions of this manuscript, Jason Lynch for providing charcoal dispersal data from the Fort Providence experimental fire, and thoughtful reviews by Christopher Carcaillet and one anonymous reviewer.

Appendix A. Sensitivity to assumptions on wind direction and the distribution of injection heights

A single injection height is an unrealistic assumption for dispersal from a buoyant plume, and it results in large skip distances at relatively low injection heights (Clark, 1988). Thus, we assume the distribution of injection heights resulting from any single fire is continuous with negative skewness (a peak at large injection heights and a long tail at smaller heights; see Peters and Higuera, 2007). We considered two other possibilities for the distribution of injection heights: (1) injection heights vary log-normally, with most particles exiting a plume at low elevations but a decreasing proportion exiting at much higher elevations and (2) injections heights vary normally, with most particles exiting a plume at a given elevation, and an equal number of particles exiting at given distances above and below this modal injection height. Together with the negatively skewed scenario, these three scenarios would result in three different cumulative distributions functions describing charcoal deposition with increasing radii from a lake (analogous to row two in Fig. 2 in the main text).

We evaluated the effects of all three assumptions by creating generic dispersal tables resulting in cumulative distribution functions that are convex ($y = r^{0.25}$), linear ($y = r^{1}$), and concave ($y = r^{1.75}$) (Fig. A1). The PCSA in each scenario, defined by the distance from which 100% of the total charcoal deposited at the lake originates, was defined by a radius of 15 km. We also tested the sensitivity of the model to assumptions on wind direction by simulating identical fire regimes with and without variable wind.

The sensitivity tests have two important results. First, for any given dispersal scenario, variation in wind direction does little to change the fundamental relationship between C_{air} and area burned at a given spatial scale (Fig. A1). While wind reduces the maximum correlation between C_{air} and area burned, as expected, the degree of this reduction is minor compared to the variations associated with the changing radii considered. Second, assumptions on the distribution of injection heights change the degree to which a charcoal record is locally biased (or distance weighted), as illustrated by the relationship between C_{air} and area burned (Fig. A1). While the radius of maximum correlation varies between scenarios, the more important difference is in the variations associated with different radii. The convex scenario is the most locally biased record, followed by the linear and concave scenarios (Fig. A1).

We chose to simulate injection heights based on the assumptions that most particles exit a plume at a high elevation and proportionally smaller numbers of particles exist at lower elevations (the negatively skewed scenario described above). This is analogous to the linear cumulative charcoal distribution, the middle-of-the-road scenario. Although we model a single fall speed (which is a function of particle size), we also use the injection height

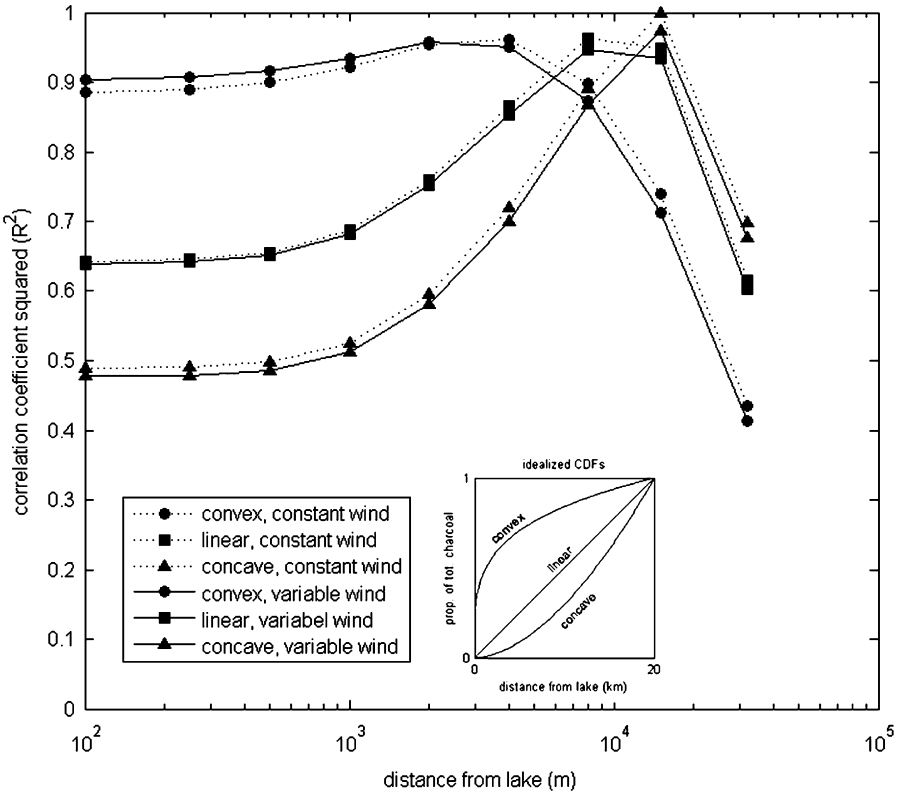

Fig. A1. Correlations of airborne charcoal accumulation and area burned at different distances from the lake for different cumulative charcoal distributions functions (CDFs; symbols, see inset) and wind scenarios (dashed or solid line, constant or variable).

distribution to implicitly represent some of the variation in particle sizes observed in empirical records (Clark et al., 1998; Lynch et al., 2004a). Smaller particles are lofted higher than larger particles, due to the same properties influencing particle dispersal. We assume that from any given 1 ha pixel in CharSim, the majority of particles injected in a plume are small and lofted to heights near the modal injection height, while a decreasing proportion of particles (assumed to be larger) are injected to proportionally smaller injection heights. The effect of particle size on subsequent transport is small and can be neglected compared to the effect on injection height (Peters and Higuera, 2007).

References

Alaska Fire Service, 2004. Alaska Fire History. Bureau of Land Management. Available online at 〈http://agdc.usgs.gov/data/blm/fire/〉.

Anderson, P.M., Brubaker, L.B., 1994. Vegetation history of northcentral Alaska: a mapped summary of Late-Quaternary pollen data. Quaternary Science Reviews 13, 71–92.

Blackford, J.J., 2000. Charcoal fragments in surface samples following a fire and the implications for interpretation of subfossil charcoal data. Palaeogeography, Palaeoclimatology, Palaeoecology 164, 33–42.

Bradbury, J.P., 1996. Charcoal deposition and redeposition in Elk Lake, Minnesota, USA. The Holocene 6, 339–344.

Brubaker, L.B., Garfinkel, H.L., Edwards, M.E., 1983. A Late Wisconsin and Holocene vegetation history from the central Brooks Range: implications for Alaskan paleoecology. Quaternary Research 20, 194–214.

Carcaillet, C., Bergeron, Y., Richard, P.J.H., Frechette, B., Gauthier, S., Prairie, Y.T., 2001a. Change of fire frequency in the eastern Canadian boreal forests during the Holocene: does vegetation composition or climate trigger the fire regime? Journal of Ecology 89, 930–946.

Carcaillet, C., Bouvier, M., Frechette, B., Larouche, A.C., Richard, P.J.H., 2001b. Comparison of pollen-slide and sieving methods in lacustrine charcoal analyses for local and regional fire history. The Holocene 11, 467–476.

Carcaillet, C., Richard, P.J.H., Asnong, H., Capece, L., Bergeron, Y., 2006. Fire and soil erosion history in East Canadian boreal and temperate forests. Quaternary Science Reviews 25, 1489–1500.

Chamberlain, A.C., 1953. Aspects of Travel and Deposition of Aerosol and Vapor Clouds. UK Atomic Energy Research Establishment Report, AERE-HP/R 1261, Harwell, Berkshire, UK, 33pp.

Clark, J.S., 1988. Particle motion and the theory of charcoal analysis: source area, transport, deposition, and sampling. Quaternary Research 30, 67–80.

Clark, J.S., 1990. Fire and climate change during the last 750 yr in northwestern Minnesota. Ecological Monographs 60, 135–159.

Clark, J.S., Royall, P.D., 1995a. Particle-size evidence for source areas of charcoal accumulation in Late Holocene sediments of eastern North American lakes. Quaternary Research 43, 80–89.

Clark, J.S., Royall, P.D., 1995b. Transformation of a northern hardwood forest by aboriginal (Iroquois) fire: charcoal evidence from Crawford Lake, Ontario, Canada. The Holocene 5, 1–9.

Clark, J.S., Royall, P.D., 1996. Local and regional sediment charcoal evidence for fire regimes in presettlement north-eastern North America. Journal of Ecology 84, 365–382.

Clark, J.S., Patterson, W.A., 1997. Background and local charcoal in sediments: scales of fire evidence in the paleorecord. In: Clark, J.S., Cachier, H., Goldammer, J.G., Stocks, B.J. (Eds.), Sediment Records of Biomass Burning and Global Change. Springer, New York, pp. 23–48.

Clark, J.S., Royall, P.D., Chumbley, C., 1996. The role of fire during climate change in an eastern deciduous forest at Devil's Bathtub, New York. Ecology 77, 2148–2166.

Clark, J.S., Lynch, J.A., Stocks, B.J., Goldammer, J.G., 1998. Relationships between charcoal particles in air and sediments in west-central Siberia. The Holocene 8, 19–29.

Clark, J.S., Grimm, E.C., Lynch, J., Mueller, P.G., 2001. Effects of Holocene climate change on the C4 grassland/woodland boundary in the Northern Plains, USA. Ecology 82, 620–636.

Cleveland, W.S., 1979. Robust locally weighted regression and smoothing scatterplots. Journal of the American Statistical Association 74, 829–836.

Enache, M.D., Cumming, B.F., 2006. Tracking recorded fires using charcoal morphology from the sedimentary sequence of Prosser Lake, British Columbia (Canada). Quaternary Research 65, 282–292.

Gardner, J.J., Whitlock, C., 2001. Charcoal accumulation following a recent fire in the Cascade Range, northwestern USA, and its relevance for fire-history studies. The Holocene 11, 541–549.

Gavin, D.G., Brubaker, L.B., Lertzman, K.P., 2003. An 1800-year record of the spatial and temporal distribution of fire from the west coast of Vancouver Island, Canada. Canadian Journal of Forest Research 33, 573–586.

Gavin, D.G., Hu, F.S., Lertzman, K., Corbett, P., 2006. Weak climatic control of stand-scale fire history during the Late Holocene. Ecology 87, 1722–1732.

Hallett, D.J., Lepofsky, D.S., Mathewes, R.W., Lertzman, K.P., 2003. 11,000 years of fire history and climate in the mountain hemlock rain forests of southwestern British Columbia based on sedimentary charcoal. Canadian Journal of Forest Research 33, 292–312.

Higuera, P.E., 2006. Late Glacial and Holocene fire history in the southcentral Brooks Range, Alaska: direct and indirect impacts of climatic change on fire regimes. Ph.D. Dissertation, University of Washington, Seattle.

Higuera, P.E., Sprugel, D.G., Brubaker, L.B., 2005. Reconstructing fire regimes with charcoal from small-hollow sediments: a calibration with tree-ring records of fire. The Holocene 15, 238–251.

Kasischke, E.S., Williams, D., Barry, D., 2002. Analysis of the patterns of large fires in the boreal forest region of Alaska. International Journal of Wildland Fire 11, 131–144.

Long, C.J., Whitlock, C., Bartlein, P.J., Millspaugh, S.H., 1998. A 9000-year fire history from the Oregon Coast Range, based on a high-resolution charcoal study. Canadian Journal of Forest Research 28, 774–787.

Lynch, J.A., Clark, J.S., Bigelow, N.H., Edwards, M.E., Finney, B.P., 2002. Geographic and temporal variations in fire history in boreal ecosystems of Alaska. Journal of Geophysical Research 108, FFR8-1–FFR8-17.

Lynch, J.A., Clark, J.S., Stocks, B.J., 2004a. Charcoal production, dispersal and deposition from the Fort Providence experimental fire: interpreting fire regimes from charcoal records in boreal forests. Canadian Journal of Forest Research 34, 1642–1656.

Lynch, J.A., Hollis, J.L., Hu, F.S., 2004b. Climatic and landscape controls of the boreal forest fire regime: Holocene records from Alaska. Journal of Ecology 92, 447–489.

MacDonald, G.M., Larsen, C.P.S., Szeicz, J.M., Moser, K.A., 1991. The reconstruction of boreal forest fire history from lake sediments: a comparison of charcoal, pollen, sedimentological, and geochemical indices. Quaternary Science Reviews 10, 53–71.

Marlon, J., Bartlein, P.J., Whitlock, C., 2006. Fire-fuel-climate linkages in the northwestern USA during the Holocene. The Holocene 16, 1059–1071.

Mohr, J.A., Whitlock, C., Skinner, C.N., 2000. Postglacial vegetation and fire history, eastern Klamath Mountains, California, USA. The Holocene 10, 587–602.

Ohlson, M., Tryterud, E., 2000. Interpretation of the charcoal record in forest soils: forest fires and their production and deposition of macroscopic charcoal. The Holocene 10, 519–525.

Peters, M.E., Higuera, P.E., 2007. Quantifying the source area of macroscopic charcoal with a particle dispersal model. Quaternary Research 67, 304–310.

Pisaric, M.F.J., 2002. Long-distance transport of terrestrial plant material by convection resulting from forest fires. Journal of Paleolimnology 28, 349–354.

Samsonov, Y.N., Joutsenogii, K.P., Makarov, V.I., Ivanov, A.V., Ivanov, V.A., McRae, D.J., Conard, S.G., Baker, S.P., Ivanova, G.A., 2005. Particulate emissions from fires in central Siberian Scots pine forests. Canadian Journal of Forest Research 35, 2207–2217.

Sugita, S., 1993. A model of pollen source area for an entire lake surface. Quaternary Research 39, 239–244.

Sutton, O.G., 1947. The theoretical distribution of airborne pollution from factory chimneys. Quarterly journal of The Royal Meteorological Society 73, 426–436.

Taylor, S.W., Wotton, B.M., Alexander, M.E., Dalrymple, G.N., 2004. Variation in wind and crown fire behavior in a northern jack pine-black spruce forest. Canadian Journal of Forest Research 34, 1561–1576.

Tinner, W., Hofstetter, S., Zeugin, F., Conedera, M., Wohlgemuth, T., Zimmermann, L., Zweifel, R., 2006. Long-distance transport of macroscopic charcoal by an intensive crown fire in the Swiss Alps—implications for fire history reconstruction. Holocene 16, 287–292.

Wein, R.W., Burzynski, M.P., Sreenivasa, B.A., Tolonen, K., 1987. Bog profile evidence of fire and vegetation dynamics since 3000 years BP in the Acadian Forest. Canadian Journal of Botany 65, 1180–1186.

Whitlock, C., Anderson, R.S., 2003. Fire history reconstructions based on sediment records from lakes and wetlands. In: Veblen, T.T., Baker, W.L., Montenegro, G., Swetnam, T. (Eds.), Fire and Climatic Change in Temperate Ecosystems of the Western Americas. Springer, New York, pp. 3–31.

Whitlock, C., Larsen, C., 2001. Charcoal as a fire proxy. In: Smol, J.P., Birks, H.J.B., Last, W.M. (Eds.), Tracking Environmental Change Using Lake Sediments. Kluwer Academic Publisher, Dordrecht.

Whitlock, C., Millspaugh, S.H., 1996. Testing the assumptions of fire-history studies: an examination of modern charcoal accumulation in Yellowstone National Park, USA. The Holocene 6, 7–15.

Whitlock, C., Skinner, C.N., Bartlein, P., Minckley, T., Mohr, J.A., 2004. Comparison of charcoal and tree-ring records of recent fires in the eastern Klamath Mountains, California, USA. Canadian Journal of Forest Research 34, 2110–2121.

Zar, J.H., 1999. Biostatistical Analysis. Prentice-Hall, Upper Saddle River, NJ.